



TO THE EDITOR:

Primary cytotoxic T-cell lymphomas harbor recurrent targetable alterations in the JAK-STAT pathway

Katie Lee,^{1,2,*} Mark G. Evans,^{3,*} Lei Yang,⁴ Spencer Ng,¹ Caroline Snowden,^{1,2} Michael Khodadoust,^{5,6} RYanne A. Brown,^{6,7} Nicholas A. Trum,⁸ Christiane Querfeld,⁸ Linda T. Doan,⁹ Jinming Song,¹⁰ Hailing Zhang,¹⁰ Alejandro A. Gru,¹¹ Gary S. Wood,¹² David A. Wada,^{13,14} Vignesh Shanmugam,³ Paul L. Haun,¹⁵ Jon C. Aster,³ Lyn M. Duncan,¹⁶ Joan Guitart,¹ David M. Weinstock,⁴ Valentina Nardi,¹⁶ and Jaehyuk Choi^{1,2,17,18}

¹Department of Dermatology and ²Department of Biochemistry and Molecular Genetics, Northwestern University Feinberg School of Medicine, Chicago, IL; ³Department of Pathology, Brigham and Women's Hospital and ⁴Department of Medical Oncology, Dana-Farber Cancer Institute, Harvard Medical School, Boston, MA; ⁵Division of Oncology, Department of Medicine ⁶Department of Dermatology and ⁷Department of Pathology, Stanford University School of Medicine, Stanford, CA; ⁸Department of Dermatology, City of Hope National Medical Center, Duarte, CA; ⁹Department of Dermatology, University of California, Irvine, Irvine, CA; ¹⁰Department of Pathology, H. Lee Moffitt Cancer Center & Research Institute, Tampa, FL; ¹¹Department of Pathology, University of Virginia, Charlottesville, VA; ¹²Department of Dermatology, University of Wisconsin, Madison, WI; ¹³Department of Dermatology and ¹⁴Huntsman Cancer Institute, University of Utah Health Sciences Center, Salt Lake City, UT; ¹⁵Penn Cutaneous Lymphoma Program, Department of Dermatology, Perelman Center for Advanced Medicine, Perelman School of Medicine at the University of Pennsylvania, Philadelphia, PA; ¹⁶Department of Pathology, Massachusetts General Hospital, Harvard Medical School, Boston, MA; ¹⁷Robert H. Lurie Comprehensive Cancer Center, Northwestern University, Chicago, IL; and ¹⁸Center for Genetic Medicine, Northwestern University Feinberg School of Medicine, Chicago, IL

Cytotoxic cutaneous T-cell lymphomas (CTCLs) are a collection of uncommon but highly aggressive cancers of skin-homing cytotoxic T cells. These include the established World Health Organization (WHO) entity primary cutaneous $\gamma\delta$ T-cell lymphomas (PCGDTLs), the provisional WHO entity primary cutaneous CD8⁺ aggressive epidermotropic T-cell lymphoma (PCAETCL), and samples that do not currently fit a specific WHO category, which we refer to as cytotoxic CTCL-NOS (not otherwise specified).¹

All 3 entities present with ulcerated skin lesions and express at least 1 cytotoxic enzyme by histopathology (supplemental Figure 1, available on the *Blood* Web site). These cytotoxic CTCL entities are clinically similar.^{2,3} There are no statistically significant differences in clinical presentation, survival, or response to therapy.^{2,3} Median survival across all 3 cytotoxic CTCL subtypes has been reported to be from 12 to 15 months.^{3,4} Because of their dismal clinical outcomes, greater insights into disease pathogenesis are needed.

We recently defined the landscape of PCGDTLs.⁵ However, little is known about the other cytotoxic CTCLs. A recent whole-genome sequencing (WGS) study of 12 PCAETCLs found recurrent *JAK2* fusions in 3 PCAETCLs.⁶ Otherwise, there is little known about these aggressive cancers.

To bridge this knowledge gap, we obtained 35 cases of cytotoxic CTCLs. All cases expressed a pan T-cell marker and at least 1 cytotoxic enzyme (TIA-1, perforin, or granzyme B). Cases were obtained from 10 academic institutions (Massachusetts General Hospital, Brigham and Women's Hospital, Northwestern, Stanford, University of Utah, University of Pennsylvania, University of Wisconsin–Madison, Moffitt Cancer Center, University of California–Irvine, City of Hope). All slides were reviewed in a blinded manner by 2 expert dermatopathologists (L.M.D. and J.G.).

All PCGDTLs expressed the γ or δ T-cell receptor. All 9 PCAETCLs expressed CD8 and had full-thickness epidermotropism. The 20 CTCL-NOSs did not meet criteria for PCAETCL because they were either CD8⁻, did not have full-thickness epidermal involvement, or had mixed histological features characteristic of other CTCLs (Table 1). Consistent with recent reports,³ there were no statistically significant differences in sites of disease, age, or sex between PCAETCLs and CTCL-NOSs in our cohort (Fisher's exact test). Both PCAETCL and CTCL-NOS had aggressive clinical courses. Median survivals were 12.2 months and 11 months, respectively (Figure 1A).

To identify oncogenic gene fusions, we performed a clinically validated targeted RNA sequencing (RNA-Seq) assay using anchored multiplexed polymerase chain reaction (PCR) technology,⁷ the Archer Heme Fusion assay, on 6 PCGDTLs, 6 PCAETCLs, and 12 CTCL-NOSs formalin-fixed paraffin-embedded (FFPE) samples. Surprisingly, all 6 PCAETCLs harbored a kinase gene fusion; 5 had a *JAK2* fusion, and one had a novel *ABL1* fusion. In contrast, none of the CTCL-NOSs or PCGDTLs expressed a kinase fusion (Figure 1B).

To investigate this further, we performed WGS and/or RNA-Seq on 3 additional PCAETCLs (1 fresh frozen and 2 FFPE) and 7 CTCL-NOSs (4 fresh frozen and 3 FFPE). The WGS and RNA-Seq were prepared and analyzed as previously described.⁵ We also added custom probes spanning *JAK2* to enrich our RNA-Seq for *JAK2* fusions. Recently, we performed a comprehensive genomic analysis of PCGDTLs that identified mutations in *JAK/STAT*, *MYC*, and *MAPK* pathways.⁵ Thus, we did not pursue additional molecular studies on this cohort.

This analysis identified *JAK2* fusions in all additional 3 PCAETCLs (Figure 1B). None of the additional CTCL-NOSs harbored an oncogenic fusion. Collectively, PCAETCLs in our cohort harbored

Table 1. Histological and clinical features of cytotoxic CTCLs

Case	WHO criteria		Fusion result	Demographic features			Clinical outcomes					
	$\gamma\delta$ TCR	CD8 ⁺		Epidermis	Assay	Transcript	Age, y	Sex	Race	Status	Skin involvement	Survival
PCAETCL												
NU1	NEG	POS	1.5 (P)	NGS	KHDRBS1-JAK2	69	M	AA	DOD	HN, T, E	15	
NU2	NEG	POS	2 (P)	Archer	CAPRIN1-JAK2	46	M	M	AWD	HN, T, G, E	26	
NU3	NEG	POS	2.5	NGS	PICALM-JAK2	84	M	C	AWD	G, T, E	26	
NU4	NEG	POS	3	NGS	PICALM-JAK2	31	M	H	AWOD*	HN, T, O, E	3	
PE12	NEG	POS	1.5 (P)	Archer	PCM1-JAK2	67	M	C	N/A	HN, T, G, E	12	
MGH3	NEG	POS	3	Archer	CAPRIN1-JAK2	69	M	C	DOD	T, E	19	
MOF4	NEG	POS	1.5 (P)	Archer	STAT3-JAK2	80	F	C	DOD	HN, T, E	7	
WIS5	NEG	POS	1.5 (P)	Archer	SELENO1-ABL1	88	M	C	DOD	T, E	2	
MGH6	NEG	POS	1.5 (P)	Archer	PCM1-JAK2	75	M	N/A	N/A	HN, T, E	9	
CD8⁺/CD4⁻ cytotoxic CTCL-NOS												
NU5	NEG	NEG	3	Archer	Negative	75	F	C	AWD	HN	39	
NU6	NEG	NEG	2.5	NGS	Negative	20	M	AA	DOD	HN, T, E	0	
NU7	NEG	NEG	1	NGS	Negative	75	F	C	AWD	HN, T, E	35	
NU8	NEG	NEG	2	Archer	Negative	67	M	C	AWD	E	8	
NU9	NEG	NEG	0	NGS	Negative	47	F	C	AWD	HN, T, E	11	
NU10	NEG	NEG	1 (MF)	Archer	Negative	45	M	C	AWD	T, G, E	36	
NU11	NEG	NEG	2	NGS	Negative	61	M	C	DOD	HN, E	21	
NU15	NEG	NEG	3	Archer	Negative	89	F	C	AWD	HN	8	
NU13	NEG	NEG	2	NGS	Negative	86	M	C	DOD	T, E	20	
NU14	NEG	NEG	2	NGS	Negative	63	M	C	DOD	HN, T, E	14	

Assays used for fusion detection were Archer or next-generation sequencing (NGS) methods. Archer (Heme fusion assay) is a custom-targeted anchored multiplex PCR-based RNA-seq assay for gene fusion detection. Fusions from RNA-seq or WGS were discovered by STAR-Fusion19 followed by manual inspection by WGS/RNA-Seq reads. Survival is reported in months from date of diagnosis to date of death (or hematopoietic stem cell transplant). Race: A, Asian; AA, African American; C, Caucasian; M, Middle Eastern; H, Hispanic. Status: AWD, alive without disease; AWOD, died of other cause; DOD, died of disease. Skin involvement: E, extremities; G, genital; HN, head/neck; O, oral mucosa; T, trunk. Epidermis density is described as 0, very low epidermal infiltrate density of the lymphoma cells; 1, low epidermal infiltrate density of the lymphoma cells; 2, intermediate density of lymphoma cells; 3, high density of lymphoma cells. M, mixed features, describing a histological pattern that have features of mycosis fungoides (MF), such as Pautrier microabscesses or lichenoid infiltrates; N, Neurotropism, neural invasion of lymphoid infiltrates NEG, negative for expression determined by immunohistochemistry (IHC); P, pagetoid, describing a pattern of lymphocytic infiltration where it is densest at the basal layer, and infiltration density becomes less sparse, but still present, at the top layer of the epidermis; POS, positive for expression determined by IHC; SUBSET, a subset of the population was positive for expression determined by IHC; TCR, T-cell receptor; VAR, variable expression determined by IHC. *Hematopoietic stem cell transplant.

Table 1. (continued)

Case	WHO criteria		Fusion result		Demographic features			Clinical outcomes			
	$\gamma\delta$ TCR	CD8 ⁺	Epidermis	Assay	Transcript	Age, y	Sex	Race	Status	Skin involvement	Survival
CD8⁺ cytotoxic CTL-NOS that did not meet criteria for PCAETCL											
NU12	NEG	VAR	2 (N)	Archer	INTS4-TP63	76	M	H	AWD	HN, E	7
NU16	NEG	POS	1	NGS	Negative	72	M	C	DOD	HN, T, E	1
BWH2	NEG	POS	0	Archer	Negative	64	M	C	AWD	HN, E	3
PE9	NEG	POS	0.5	Archer	Negative	75	M	C	AWD	HN, T, O, E	43
PET0	NEG	POS	0.5 (MF)	Archer	Negative	67	M	AA	N/A	HN, T, G, E	4
PET1	NEG	POS	0.5 (MF)	Archer	Negative	82	M	C	N/A	E	7
PET4	NEG	POS	1.5	Archer	Negative	52	F	C	DOD	T, E	37
ST15	NEG	POS	1	Archer	Negative	75	M	A	DOD	HN, T, O, E	7.9
UC18	NEG	POS	1.5	Archer	Negative	63	M	C	DOD	HN, T, E	14
UT22	NEG	POS	2 (MF)	NGS	Negative	70	M	C	AWD	HN, T, E	10
PCGDTL											
COH16	POS	NEG	2	Archer	Negative	78	M	C	DOD	T, G, E	22
COH17	POS	SUBSET	0	Archer	Negative	68	M	C	DOD	E	15
COH18	POS	NEG	0	Archer	Negative	63	M	C	DOD	T, E	1
COH19	POS	NEG	2	Archer	Negative	81	M	C	DOD	HN, T, G, E	50
COH20	POS	NEG	2 (MF)	Archer	Negative	75	F	C	AWD	T, E	15
COH21	POS	POS	1.5	Archer	Negative	40	M	C	AWD	HN, T, E	64

Assays used for fusion detection were Archer or next generation sequencing (NGS) methods. Archer (Heme fusion assay) is a custom-targeted anchored multiplex PCR-based RNA-seq assay for gene fusion detection. Fusions from RNA-seq or WGS were discovered by STAR-Fusion19 followed by manual inspection by WGS/RNA-Seq reads. Survival is reported in months from date of diagnosis to date of death (or hematopoietic stem cell transplant). Race: A, Asian; AA, African American; C, Caucasian; M, Middle Eastern; H, Hispanic. Status: AWD, alive with disease; AWOD, alive without disease; DOC, died of other cause; DOD, died of disease. Skin involvement: E, extremities; G, genitals; HN, head/neck; O, oral mucosa; T, trunk. Epidermis density is described as 0, very low epidermal infiltrate density of the lymphoma cells; 1, low epidermal density of lymphoma cells; 2, intermediate density of lymphoma cells; 3, high density of lymphoma cells. M, mixed features, describing a histological pattern that have features of mycosis fungoides (MF), such as Pautrier microabscesses or lichenoid infiltrates; N, Neurotropism, neural invasion of lymphoid infiltrates. NEG, negative for expression determined by immunohistochemistry (IHC); P, pagetoid, describing a pattern of lymphocytic infiltration where it is densest at the basal layer, and infiltration density becomes less sparse, but still present, at the top layer of the epidermis; POS, positive for expression determined by IHC; SUBSET, a subset of the population was positive for expression determined by IHC; TCR, T-cell receptor; VAR, variable expression determined by IHC. *Hematopoietic stem cell transplant.

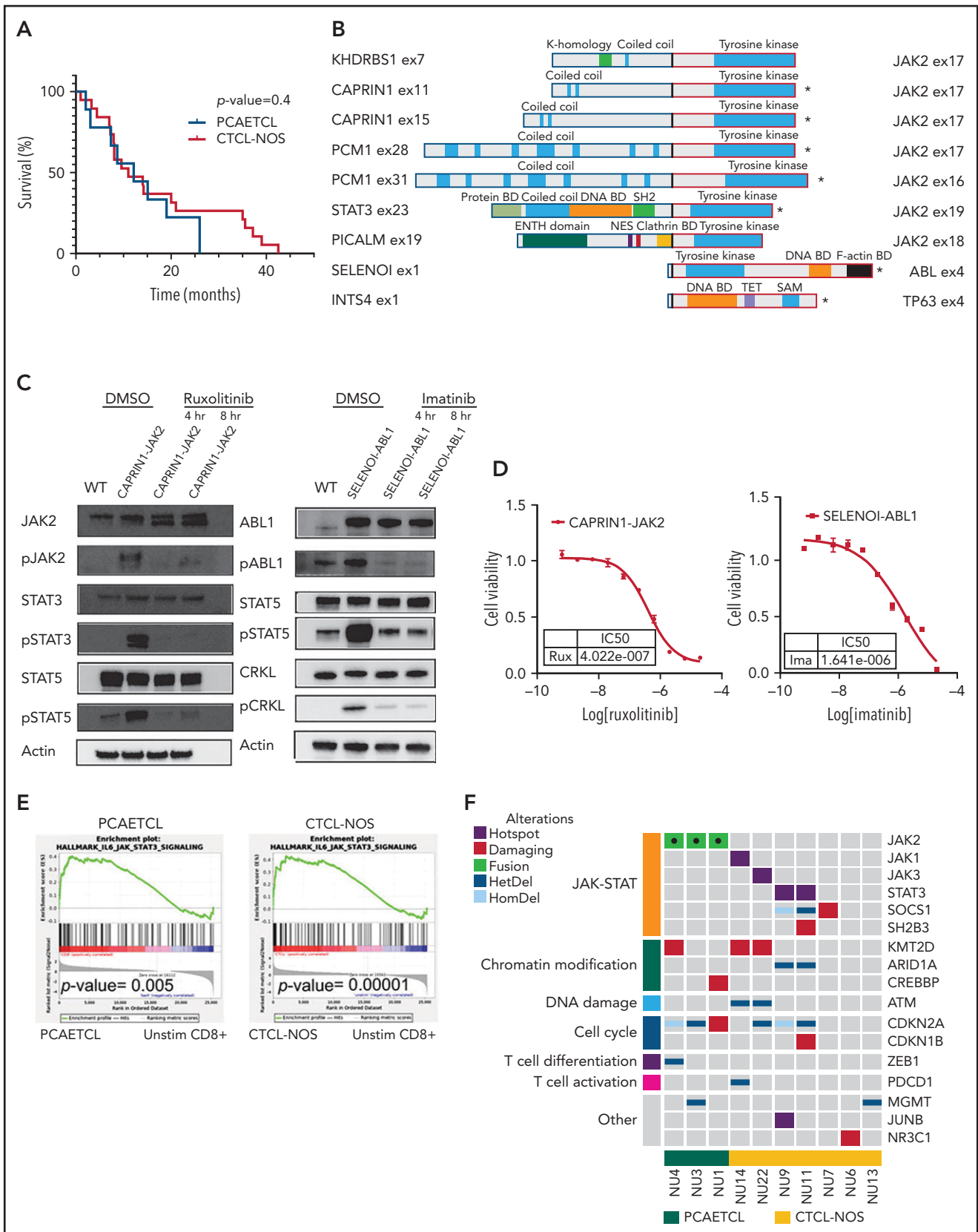


Figure 1. Cytotoxic CTLs harbor targetable mutations that activate the JAK-STAT pathway. (A) Survival curves for PCAETCL and CTCL-NOS were generated and analyzed with Log-rank (Mantel-Cox) test. (B) Summary of all fusions and their known domains. *Transcripts detected by the Archer assay. The rest were identified by WGS and/or RNA-Seq. Breakpoints are denoted with bold, black junctions. Clathrin BD, Clathrin binding domain; DNA BD, DNA binding domain; Protein BD, binding domain; NES, nuclear export signaling domain; TET, tetramerization domain. (C) Western blots of pathway targets in CAPRIN1-JAK2 and SELENOI-ABL1-expressing Ba/F3. Cells were transduced with novel fusion genes or wild-type kinase controls and treated with either vehicle or indicated drug for indicated times. Antibodies used

JAK2 fusions reported in other cancers (*PCM1-JAK2* and *STAT3-JAK2*),⁸⁻¹⁰ JAK2 fusions recently reported for PCAETCL (*KHDRBS1-JAK2*),⁶ and 3 fusions not previously described in any cancer (*PICALM-JAK2*, *CAPRIN1-JAK2*, and *SELENOI-ABL1*) (Figure 1B).

All JAK2 translocations involved introns 15 to 18, preserved the catalytic domain, but lost the upstream FERM, SH2, and the regulatory pseudokinase domains. The *ABL1* fusion also retained its catalytic tyrosine kinase domain but lost its N-terminal regulatory SH2 and SH3 domains. This fusion is analogous to *NPM1-ABL1*, but not *BCR-ABL1* fusions, which also lose their SH2/SH3 domains.

To functionally validate these fusions, we obtained cDNA for *CAPRIN1*, *JAK2*, and *ABL1* (Horizon; Addgene). We cloned the fusion genes into pMSCVpuro-DEST vector (Addgene). We transduced Ba/F3 cells with retrovirus encoding *CAPRIN1-JAK2*, *SELENOI-ABL1*, or wild-type *JAK2* or *ABL1*. Like other oncogenes,¹¹ both gene fusions, but not wild-type kinases, conferred IL-3-independent growth (supplemental Figure 2A-B). Both *CAPRIN1-JAK2* and *SELENOI-ABL1* increased phosphorylation of targets downstream in their respective signaling cascades (Figure 1C). For *CAPRIN1-JAK2*, these include phospho-JAK2 (pJAK2), pSTAT3, and pSTAT5. For *SELENOI-ABL1*, these include pABL, pSTAT5, and pCRKL.

Next, we assessed their potential targetability. The JAK1/JAK2 inhibitor ruxolitinib decreased pJAK2, pSTAT3, and pSTAT5 and decreased viability of cells expressing *CAPRIN1-JAK2* fusions (50% inhibitory concentration [IC₅₀] = 402.2 nM). Similarly, imatinib inhibited *SELENOI-ABL1*-dependent phosphorylation cascades and viability (IC₅₀ = 1641 nM) (Figure 1D). As previously shown for *NPM1-ABL1*, the allosteric inhibitor asciminib that binds a myristoyl site in *ABL1*¹² had no effect on *SELENOI-ABL1* fusion expressing cells (data not shown).

We then analyzed the RNA-Seq data for transcriptional evidence of JAK-STAT activation. As expected, gene set enrichment analysis demonstrated a significant upregulation of a JAK-STAT gene signature in PCAETCLs (*P* value = .005) compared with unstimulated CD8⁺ T cells (Figure 1E). To confirm this observation at the protein level, we performed IHC for pSTAT3 (clone D3A7, Cell Signaling Technology) on 5 samples. These include 1 PCAETCL expressing the *SELENOI-ABL1* fusion (predicted to phosphorylate pSTAT5 but not pSTAT3), 3 PCAETCL samples with JAK2 fusions (*PCM1-JAK2* and *STAT3-JAK2*), and a CTCL-NOS without a known JAK-STAT mutation. As expected, we found pSTAT3 in the 3 samples with JAK2 fusions but not in the other samples (supplemental Figure 3).

Next, we analyzed our WGS data as previously described¹³ (supplemental Table 1). Five of 7 (71%) CTCL-NOSs had a somatic

single nucleotide variant (SSNV) predicted to activate JAK-STAT signaling, including hotspot mutations in *STAT3*, p.D661Y (NU9) and p.P714L (NU11), *JAK1*, p.G1097D (NU14), *JAK3*, p.P906S (UT22), a damaging mutation in *SOCS1*, p.Q108* (NU7), and a *SH2B3* splice site mutation (NU11). As previously reported, we found *CDKN2A* mutations in all PCAETCLs.⁶ These were also present in 43% of CTCL-NOSs (Figure 1F). Moreover, CTCL-NOSs and/or PCAETCLs harbored mutations in other genes recurrently mutated in CTCL,^{11,14} including chromatin modification (*ARID1A*, *KMT2D*, *CREBBP*), cell cycle (*CDKN1B*), and DNA damage genes (*ATM*). Consistent with their genetics, CTCL-NOSs also had significant enrichment of the JAK-STAT gene set in their RNA-Seq data (*P* = .00001). Despite the negative pSTAT3 IHC in the 1 CTCL-NOS sample, these data suggest transcriptional activation of ≥1 STATs in this disease cohort.

Our observations have immediate clinical importance for both classification and treatment. Strikingly, all 9 PCAETCLs in our series harbored kinase fusions, suggesting that these fusions may be a disease-defining characteristic. At the same time, the majority of CTCL-NOSs harbor SSNVs that activate JAK/STAT signaling. Although both cancers may require oncogenic JAK-STAT signaling, the literature suggests variable genotype-driven responses to JAK inhibitors. JAK2 fusions predict exceptional response to small molecule inhibitors, while responses in cases with activating SSNVs are variable.¹⁵ A recent study of ruxolitinib in peripheral T-cell lymphoma and CTCLs reported responses in 23% of patients with activating JAK/STAT SSNVs.¹⁶

The reasons underlying the genetic differences between PCAETCLs and CTCL-NOSs remain unclear. It is possible that these kinase fusions and JAK/STAT SSNVs have subtle molecular differences. Nonetheless, our data add to the growing body of literature wherein molecular differences between tumors correlate with histological patterns.^{17,18}

We received informed consent for these patients in accordance with Northwestern Institutional Review Board standards.

Acknowledgments

The authors acknowledge the patients, the Northwestern Skin Disease Research Center, the Northwestern University Research Computing Services, and Admera Health.

This work was supported by National Institutes of Health (NIH), National Institute of Arthritis Musculoskeletal and Skin Diseases grant P30-AR066524 (G.S.W.), NIH, National Cancer Institute grants R35-CA231958 (D.M.W.) and P01-CA248384 (D.M.W.), Leukemia and Lymphoma Society grant SCOR 7026-21 (D.M.W.), Leukemia and Lymphoma Society grant 1377-21 (J.C.), and Doris Duke Charitable Fund grant 2020132 (J.C.).

Figure 1 (continued) against JAK2 (#3230), pJAK2 (#3771), cABL (#2862), pABL (#2868), STAT3 (#9139), pSTAT3 (#9145), STAT5 (#94205), pSTAT5 (#4322), CRKL (#38710), and pCRKL (#3181) were obtained from Cell Signaling Technology. (D) Cell viability assay to determine IC₅₀ values of ruxolitinib and imatinib in *CAPRIN1-JAK2*-expressing Ba/F3 and *SELENOI-ABL1*-expressing Ba/F3, respectively. We cultured 0.1 × 10⁶ cells per mL with inhibitors or vehicle in a 384-well plate. After 48 hours, Cell-titer Glo (CTG) luminescent reagent (Promega) was added. Luminescence was read by EnVision Multilabel Reader (PerkinElmer). Each data point was quantified in quadruplicate. Cell line experiments were repeated at least in triplicate. Dose response curves were generated with GraphPad. (E) Gene set enrichment analysis of Molecular Signatures Database Hallmark IL-6-mediated JAK-STAT signaling in PCAETCL compared with unstimulated (unstim) CD8⁺ T cells and CTCL-NOS compared with unstimulated CD8⁺ T cells. *P* values were .005 and .00001, respectively. (F) Oncoplot of PCAETCL and CTCL-NOS. Fusion events were called using STAR-Fusion¹⁹ and confirmed via manual inspection of sequencing data. Splice site, frameshift, or nonsense mutations were called as damaging mutations in known tumor suppressors. Hotspot mutations were recurrent amino acid alterations. Copy number deletions for focal deletion (<5 Mb). DMSO, dimethyl sulfoxide; ENTH, epsilon N-terminal homology domain; HetDel, heterozygous copy number deletion; HomDel, biallelic deletions; WT, wild type.

Authorship

Contribution: K.L., J.G., D.M.W., V.N., and J.C. wrote the manuscript; K.L. and C.S. performed sequencing and bioinformatics analyses; L.Y. performed the functional assays; K.L., M.G.E., S.N., M.K., R.A.B., N.T., C.Q., L.T.D., J.S., H.Z., A.A.G., G.S.W., D.A.W., V.S., P.L.H., and V.N. provided the samples and clinical data at their respective centers; J.C.A. and V.N. performed the immunohistochemistry staining; L.M.D. and J.G. reviewed histology images; and K.L., M.G.E., and J.G. analyzed the clinical data.

Patient samples and clinical information were collected in accordance with the Institutional Review Board of Northwestern University (STU00009443).

Conflict-of-interest disclosure: The authors declare no competing financial interests.

ORCID profiles: K.L., 0000-0002-9919-4962; M.G.E., 0000-0001-9358-9843; S.N., 0000-0002-1251-4514; M.K., 0000-0001-9061-7351; R.A.B., 0000-0001-9099-7227; N.A.T., 0000-0002-3256-4340; C.Q., 0000-0001-9698-5809; D.M.W., 0000-0002-8724-3907; J.C., 0000-0003-2379-2226.

Correspondence: Valentina Nardi, Massachusetts General Hospital, Harvard Medical School, Warren 2, 55 Fruit St, Boston, MA 02114; e-mail: vnardi@partners.org; and Jaehyuk Choi, Robert H. Lurie Comprehensive Cancer Center, Northwestern University, 303 E. Superior St, Room 5-115, Chicago, IL 60611; e-mail: jaehyuk.choi@northwestern.edu.

Footnotes

Submitted 16 May 2020; accepted 29 July 2021; prepublished online on *Blood* First Edition 25 August 2021.

*K.L. and M.G.E. contributed equally to this study.

For samples in accordance with institutional review board, DNA/RNA sequencing will be deposited into database of Genotypes and Phenotypes. The database of Genotypes and Phenotypes accession number is phs002456.v1.p1.

The online version of this article contains a data supplement.

There is a *Blood* Commentary on this article in this issue.

REFERENCES

1. Willemze R, Jaffe ES, Burg G, et al. WHO-EORTC classification for cutaneous lymphomas. *Blood*. 2005;105(10):3768-3785.
2. Swerdlow SH, Campo E, Pileri SA, et al. The 2016 revision of the World Health Organization classification of lymphoid neoplasms. *Blood*. 2016;127(20):2375-2390.
3. Guitart J, Martinez-Escala ME, Subtil A, et al. Primary cutaneous aggressive epidermotropic cytotoxic T-cell lymphomas: reappraisal of a provisional entity in the 2016 WHO classification of cutaneous lymphomas. *Mod Pathol*. 2017;30(5):761-772.
4. Toro JR, Liewehr DJ, Pabby N, et al. Gamma-delta T-cell phenotype is associated with significantly decreased survival in cutaneous T-cell lymphoma. *Blood*. 2003;101(9):3407-3412.
5. Daniels J, Doukas PG, Escala MEM, et al. Cellular origins and genetic landscape of cutaneous gamma delta T cell lymphomas. *Nat Commun*. 2020;11(1):1806.
6. Bastidas Torres AN, Cats D, Out-Luiting JJ, et al. Dereglulation of JAK2 signaling underlies primary cutaneous CD8+ aggressive epidermotropic cytotoxic T-cell lymphoma [published online ahead of print 01 April 2021]. *Haematologica*. 2021.
7. Zheng Z, Liebers M, Zhelyazkova B, et al. Anchored multiplex PCR for targeted next-generation sequencing. *Nat Med*. 2014;20(12):1479-1484.
8. Reiter A, Walz C, Watmore A, et al. The t(8;9)(p22;p24) is a recurrent abnormality in chronic and acute leukemia that fuses PCM1 to JAK2. *Cancer Res*. 2005;65(7):2662-2667.
9. Sharma A, Oishi N, Boddicker RL, et al. Recurrent STAT3-JAK2 fusions in indolent T-cell lymphoproliferative disorder of the gastrointestinal tract. *Blood*. 2018;131(20):2262-2266.
10. Fernandez-Pol S, Neishaboori N, Chapman CM, et al. Two cases of mycosis fungoides with PCM1-JAK2 Fusion. *JCO Precis Oncol*. 2021; (5):646-652.
11. Kong K, Ng PK, Scott KL. Ba/F3 transformation assays. *Oncotarget*. 2017;8(22):35488-35489.
12. Adrián FJ, Ding Q, Sim T, et al. Allosteric inhibitors of Bcr-abl-dependent cell proliferation. *Nat Chem Biol*. 2006;2(2):95-102.
13. Park J, Yang J, Wenzel AT, et al. Genomic analysis of 220 CTCLs identifies a novel recurrent gain-of-function alteration in RLTPR (p.Q575E). *Blood*. 2017;130(12):1430-1440.
14. Park J, Daniels J, Wartewig T, et al. Integrated genomic analyses of cutaneous T cell lymphomas reveal the molecular bases for disease heterogeneity [published online ahead of print 11 June 2021]. *Blood*. 2021;blood.2020009655.
15. Roberts KG, Li Y, Payne-Turner D, et al. Targetable kinase-activating lesions in Ph-like acute lymphoblastic leukemia. *N Engl J Med*. 2014; 371(11):1005-1015.
16. Moskowitz A, Ghione P, Jacobsen ED, et al. Final results of a phase II biomarker-driven study of ruxolitinib in relapsed and refractory T-cell lymphoma. American Society of Hematology. Orlando, FL: *Blood*; 2019:4019
17. Echle A, Rindtorff NT, Brinker TJ, Luedde T, Pearson AT, Kather JN. Deep learning in cancer pathology: a new generation of clinical biomarkers. *Br J Cancer*. 2021;124(4):686-696.
18. Zhang H, Kalirai H, Acha-Sagredo A, Yang X, Zheng Y, Coupland SE. Piloting a Deep Learning Model for Predicting Nuclear BAP1 Immunohistochemical Expression of Uveal Melanoma from Hematoxylin-and-Eosin Sections. *Transl Vis Sci Technol*. 2020;9(2):50.
19. Haas BJ, Dobin A, Li B, Stransky N, Pochet N, Regev A. Accuracy assessment of fusion transcript detection via read-mapping and de novo fusion transcript assembly-based methods. *Genome Biol*. 2019; 20(1):213.

DOI 10.1182/blood.2021012536

© 2021 by The American Society of Hematology